Optimization and Validation of a Constrained Reconstruction Algorithm for Rapid Whole-Brain Cross-Relaxation Imaging at 3.0 Tesla

H. R. Underhill[1], C. Yuan[1], and V. L. Yarnykh[1]

[1]University of Washington, Seattle, WA, United States

Introduction: Cross-relaxation imaging (CRI) is a method for quantitative mapping of parameters describing magnetization transfer between mobile water protons (free pool) and macromolecular protons (bound pool) in tissues [1,2]. Time-efficient three-dimensional (3D) whole-brain CRI technique has been enabled at 1.5T by using the pulsed off-resonance saturation method with a limited number (four) of offset frequencies [2]. This technique determines the principle kinetic parameters of the two-pool model [3] (fraction of macromolecular protons, *f*; and the rate constant, *k*) by fitting the matrix equation describing pulsed magnetization transfer [1]. The key feature of this technique is that the transverse relaxation time of both the free (T_2^F) and bound (T_2^B) pools are constrained to reduce the number of fitted parameters and, correspondingly, enable reconstruction of *f* and *k* parametric maps from a limited number of experimental measurements. For T_2^F, the constraint is based on its approximately inverse dependence on the longitudinal relaxation rate of the free pool ($T_2^F = 0.055 / R_1^F$), and T_2^B is assumed to be constant for all tissues ($T_2^B = 11$ µs) [2]. Since relaxation properties of tissues depend on magnetic field strength, the validity of the above constraints needs to be tested for 3.0 T imaging, which becomes increasingly popular in neuroscience research.

Purpose: Validate the constrained two-parameter fit CRI reconstruction algorithm and determine the optimal constraints of T_2^F and T_2^B for whole-brain CRI at 3.0 T.

Methods: Imaging: Five healthy volunteers (4 male, 1 female, mean age 36.6 years, range 28 – 53 years) were imaged at 3.0 T (Philips Achieva, Release 2.1.1, Best, Netherlands) with a transmit/receive head coil. Four pulsed *Z*-spectroscopic data points with variable offset frequencies (Δ) of the off-resonance saturation pulse (effective flip angle 990°; Δ = 1, 2, 4, and 8 kHz; duration 19 ms) were acquired with a 3D spoiled gradient echo pulse sequence (TR/TE = 43/2.3 ms, $\alpha = 10°$) as previously described [2]. For a single volunteer (Subject A), a total of 12 data points were acquired with identical offset frequencies and timing parameters using effective flip angles of 700°, 850°, and 990°. A reference image for data normalization was obtained with Δ = 96 kHz (no MT effect is observed at this frequency) for each effective flip angle to ensure that the transmitter operates with identical gain settings. A complementary R_1 map necessary for parameter fitting was obtained using the variable flip angle (VFA) method with a 3D spoiled gradient echo sequence (TR/TE = 20/2.3 ms, α = 3, 10, 20, and 40°). All *Z*-spectroscopic and VFA images were acquired with FOV = 240x180x180 mm, matrix = 160x120x60, resolution 1.5x1.5x3.0 mm (zero-interpolated to 1.0x1.0x1.5 mm), and one signal average. Scan time was 3.33 minutes and 1.55 minutes per point for *Z*-spectroscopy and VFA, respectively. To account for effects of B_0 and B_1 heterogeneity, whole-brain B_0 and B_1 maps were acquired using previously described techniques [4,5] to establish actual off-resonance of the saturation pulse and determine actual flip angles during parameter fitting. Total scan time for the entire imaging protocol (with 4-point acquisition) was < 30 minutes.

Analysis: Parameter optimization was performed in two parts. Part 1: Four-parameter (*f*, *k*, T_2^F and T_2^B) fitting was performed with 12-point data acquired from Subject A for each of 12 anatomic locations (grey matter, *N*=5; white matter, *N*=7). Two-parameter fitting was then performed using 12-point data from Subject A while ranging T_2^F and T_2^B across a series of values. For each combination of T_2^F and T_2^B, the root-mean-square error (RMSE) was calculated between 1) acquired and theoretical data (Fig. 1A); 2) values of *f* determined by four- and two-parameter fit (Fig 1B); and 3) values of *k* determined by four- and two-parameter fit (Fig 1C). Optimal constraints for T_2^F and T_2^B were identified by the minimization of error across all differences. Once constraints for T_2^F and T_2^B were determined, Pearson's correlation coefficient, *r*, was used to compare results from the four-parameter fit and the constrained two-parameter fit. Part 2: In each of the remaining four subjects with 4-point data only, a constrained two-parameter fit (*f* and *k*) was performed in the same 12 anatomic locations across a range of values for T_2^F and T_2^B. RMSE was calculated between acquired and theoretical data and averaged across subjects (Fig. 1D). In addition, the standard deviation (SD) of *f* (Fig. 1E) and *k* (Fig. 1F) for each structure between subjects was determined and averaged across all structures. Constraints for T_2^F and T_2^B were determined by the minimization of error and standard deviation. Constraints derived from Part 1 and Part 2 were used to determine the optimal constraints for T_2^F and T_2^B. .

Table 1. Mean±SD of anatomic structures* from constrained two-parameter fit.

	k, s^{-1}	***f***, %
Globus Pallidus	2.44±0.26	7.8±0.4
Head of Caudate	1.21±0.32	6.1±0.5
Putamen	1.42±0.16	6.6±0.6
Substantia Nigra	2.09±0.47	8.2±0.4
Thalamus	1.95±0.22	7.9±1.0
Corona Radiata	3.63±0.77	11.0±0.8
Corpus Callosum, Genu	3.21±1.11	14.7±0.6
Corpus Callosum, Splenium	3.46±0.30	12.5±1.0
Frontal White Matter	3.33±0.40	11.9±0.9
Internal Capsule, Posterior Limb	3.01±0.36	11.4±0.6
Middle Cerebellar Peduncle	3.91±0.81	10.9±0.7
Occipital White Matter	3.17±0.93	10.8±0.8

*Grey matter structures in **bold**

Results: Constraints determined from Part 1 and Part 2 were identical. Optimal constraints for T_2^F and T_2^B were $0.024/R_1^F$ and 11 µs, respectively. Comparison of results from the four-parameter fit and the two-parameter fit using these constraints demonstrated a strong association for *f* (r = 0.98, p<0.001) and *k* (r = 0.91, p<0.001). Parametric *k* and *f* maps obtained by 2- and 4-parameter fit (Fig. 3) generally demonstrate good agreement, though 2-parameter fit results in clear improvement of image quality due to reduced noise. The mean±SD values for *k* and *f* for different anatomic structures obtained with optimized constraints from 4 subjects are presented in Table 1.

Discussion: Since goodness of fit between acquired and theoretical data was tolerable across a variety of T_2^F and T_2^B values, selection of appropriate constraints was primarily driven by narrow valleys of agreement between four- and two-parameter determination of *f* and *k*. The identified constraints are consistent with observations by Cercignani et al who found $T_2^F R_1^F$ to decrease by nearly 50% at 3.0 T compared to 1.5 T, while T_2^B remained relatively unchanged using a continuous wave power equivalent technique [6].

Conclusions: This study demonstrated the feasibility of whole-brain CRI at 3.0 T with a clinically acceptable scan time. To achieve correct estimates of the parameters *f* and *k* using the constrained two-parameter fitting algorithm, the constraint given by the previously determined product $T_2^F R_1^F$ at 1.5T needs to be reconsidered. The new value of the constraint $T_2^F R_1^F$ at 3.0 T reflects field dependent changes of longitudinal and transverse relaxation.

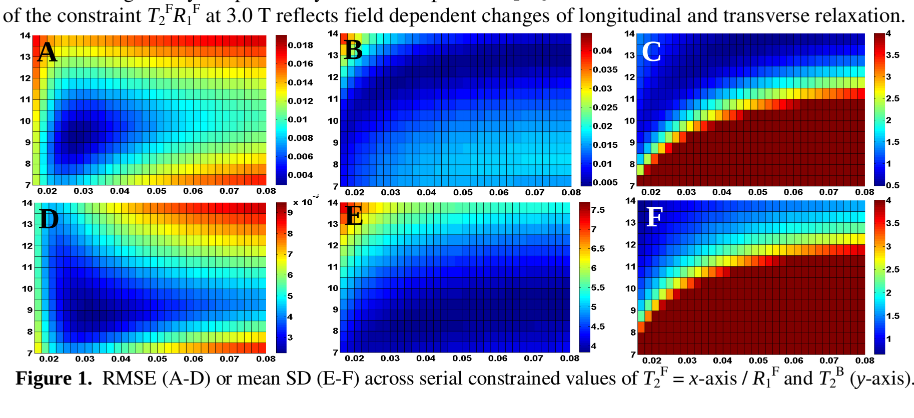

Figure 1. RMSE (A-D) or mean SD (E-F) across serial constrained values of T_2^F = *x*-axis / R_1^F and T_2^B (*y*-axis).

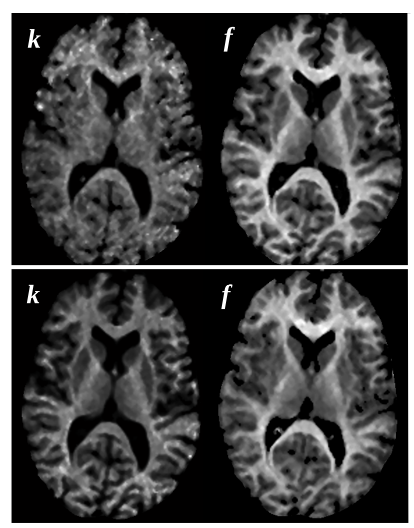

Figure 2. Axial *k* and *f*-maps from 4-parameter (top) and constrained 2-parameter fit (bottom)

References:

1. Yarnykh MRM 2002;47:929-39.
2. Yarnykh and Yuan Neuroimage 2004;23:409-24
3. Henkelman et al. MRM 1993;29:759-66
4. Skinner and Glover MRM 1997;37:628-30
5. Yarnykh MRM 2007;57:192-200
6. Cercignani et al Neuroimage 2006;31:181-86